

PACS numbers: 42.55.Rz; 42.60.Da; 42.60.Jf; 42.25.Ja
DOI: 10.1070/QE2014v044n05ABEH015440

Laser amplifier based on a neodymium glass rod 150 mm in diameter

A.A. Shaykin, A.P. Fokin, A.A. Soloviev, A.A. Kuzmin, I.A. Shaikin, K.F. Burdonov, A.V. Charukhchev, E.A. Khazanov

Abstract. **A unique large-aperture neodymium glass rod amplifier is experimentally studied. The small-signal gain distribution is measured at different pump energies. The aperture-averaged gain is found to be 2.3. The stored energy (500 J), the maximum possible pump pulse repetition rate, and the depolarisation in a single pulse and in a series of pulses with a repetition rate of one pulse per five minutes are calculated based on the investigations performed. It is shown that the use of this amplifier at the exit of the existing laser can increase the output pulse energy from 300 to 600 J.**

Keywords: *large-aperture amplifier, neodymium glass, induced birefringence, thermally induced depolarisation.*

1. Introduction

Large-aperture neodymium glass rod amplifiers have been used for a rather long time in lasers with a pulse energy of hundreds of joules [1–3]. Currently, interest in these lasers increases due to the appearance of projects aimed at the creation of multipetawatt laser complexes. These projects can be divided into three types: some of them use neodymium glass as a gain medium, other projects use Ti : sapphire (corundum with titanium) gain crystals, and third-type projects are based on parametric amplification. Neodymium glass lasers also play a key role in the second and third types, where they are used for pumping the amplifiers. The possibility of desining active elements that have a large volume and aperture and combine high optical quality with high stored energy is the main advantage of neodymium glass compared to the other available laser media. The large aperture allows the element to operate at a laser radiation intensity lower than its optical breakdown threshold in a regime of nanosecond pulses with an energy up to kilojoules. It is this energy that is required for realisation of multipetawatt projects.

High-power neodymium glass amplifiers can be designed with active elements of two geometries – rods and slabs. The advantages of rod elements are the single-pass amplification scheme, better output beam quality, compactness, and simple alignment. One more advantage of rods is the possibility of operating with a high pulse repetition rate [3, 4] owing to cooling of the side surface and compensation of optical distortions using a 90° polarisation rotator placed between two identical elements.

The factors limiting the output energy of neodymium glass lasers are optical breakdown and small-scale self-focusing [5]. Slab amplifiers may provide higher output pulse energies due to large apertures, up to 40×40 cm. At present, diameters of rod amplifiers do not exceed 10 cm, which limits the energy of 1-ns pulses at a level of about 300 J [6]. In the present work, we describe and study a scheme of a neodymium glass amplifier with a rod diameter of 15 cm.

A.A. Shaykin, A.P. Fokin, A.A. Soloviev, A.A. Kuzmin, I.A. Shaikin, K.F. Burdonov, E.A. Khazanov Institute of Applied Physics, Russian Academy of Sciences, ul. Ul'yanova 46, 603950 Nizhnii Novgorod, Russia; e-mail: shaykin@appl.sci-nnov.ru;
A.V. Charukhchev Public Limited Company 'Scientific Research Institute for Optoelectronic Instrument Engineering', POB 23, 188540 Sosnovyi Bor, Leningrad region, Russia

Received 3 March 2014; revision received 2 April 2014
Kvantovaya Elektronika **44** (5) 426–430 (2014)
Translated by M.N. Basieva

2. Amplifier design

The laser amplifier (Fig. 1) consists of a rod of neodymium-doped phosphate glass (KGSS0180) placed into a pump cavity. The rod faces are tilted at an angle of 5°; the side surface is matted.

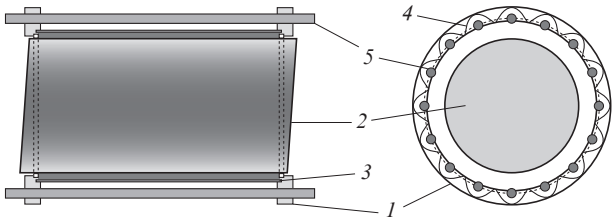

Figure 1. Laser amplifier geometry:
(*1*) amplifier housing; (*2*) active element; (*3*) quartz tube; (*4*) reflectors made of MIRO-Silver aluminium foil; (*5*) IFP8000 pump lamps.

The pump cavity is designed in the form of a metal frame (*1*) with active element (*2*), quartz tube (*3*), reflectors (*4*), and pump lamps (*5*) mounted inside. The active element (AE) and the tube are placed coaxially, and the space between them (7.5 mm) is filled with water to improve heat removal from the AE and to decrease reflection and scattering from its surface. The pump cavity design allows cooling by running water for more efficient heat removal.

The AE is pumped by 16 IFP8000 gas-discharge lamps with a discharge gap 16 mm in diameter and 250 mm long, which are positioned symmetrically along the active element axis. Reflectors placed from the external side of the lamps increase the radiation flux to the AE. The lamps are connected to four pulsed power suppliers (four lamps per each unit). The storage capacity in each power supply unit is 200 μF, the working voltage is 6–12 kV. To increase the service

life of the lamps, we use an additional preionisation circuit with a voltage of 12 kV [7].

The pump cavity was placed on a table which allowed independent alignment of the input and output faces of the AE with respect to the signal beam.

3. Measurement of the gain

The small-signal gain was measured according to the principal scheme shown in Fig. 2. The pump cavity was placed between two telescopes. The first one was used to form quasi-homogeneous intensity distribution of optical radiation over the AE aperture.

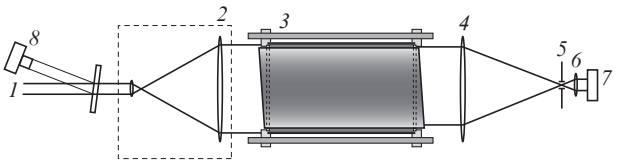

Figure 2. Scheme of measuring the laser amplifier parameters: (*1*) input beam; (*2*) telescope forming a quasi-homogeneous intensity distribution over the AE aperture; (*3*) studied amplifier; (*4*, *6*) telescope lenses relaying the AE image to the CCD camera; (*5*) accessory aperture; (*7*) 12-bit progressive scan CCD camera with a resolution of 1392×1032 pixels; (*8*) photodiode.

The pulse energy incident on the AE was measured by photodiode (*8*) to be 2 mJ at a pulse duration of 1 ns. The radiation amplified in the AE falls on a telescope, which transfers the image from the AE output face to CCD array (*7*).

To improve the measurement reliability, the most part of spontaneous emission was filtered by aperture (*5*) placed in the output telescope waist. The aperture diameter was chosen as a compromise between good spontaneous emission filtration and high-quality image relay from the AE output to the CCD array. In our experiments, the angular aperture size was 4.5×10^{-7} sr. Under these conditions, the spontaneous emission energy incident on the array was at least an order of magnitude lower than the signal beam energy.

The most part of the emission spectrum of pump lamps was cut off by a filter placed in front of the CCD camera. The small-signal gain K_0 was calculated by processing four images according to the algorithm

$$K_0 = \frac{A_1 - A_0}{I_1 - I_0},$$

where A_1 is the intensity of the amplified signal image with contributions of spontaneous emission and light of pump lamps, A_0 is the intensity of spontaneous emission and light of pump lamps at the same stored energy but in the absence of the input signal beam, I_1 is the intensity of the signal beam image without spontaneous emission and pump lamp light, and I_0 is the intensity of background illumination with allowance for the CCD array noise. The measurement error of K_0 did not exceed 8%.

The experimental distribution of the small-signal gain K_0 at a 32.4-kJ energy stored in the capacitors is shown in Fig. 3a. At a working storage energy of 48.4 kJ, the aperture-averaged gain was 2.28, which corresponds to ~500 J of energy stored in the AE. The dependence of the energy stored in the AE E_{st} on the energy in capacitors E_{el} is shown in Fig. 3b. The maximum possible energy E_{st} = 550 J is achieved at E_{el} = 62 kJ, but the probability of breakdown of lamps in this case is 20%. Therefore, the amplifier cannot be used in this operation regime.

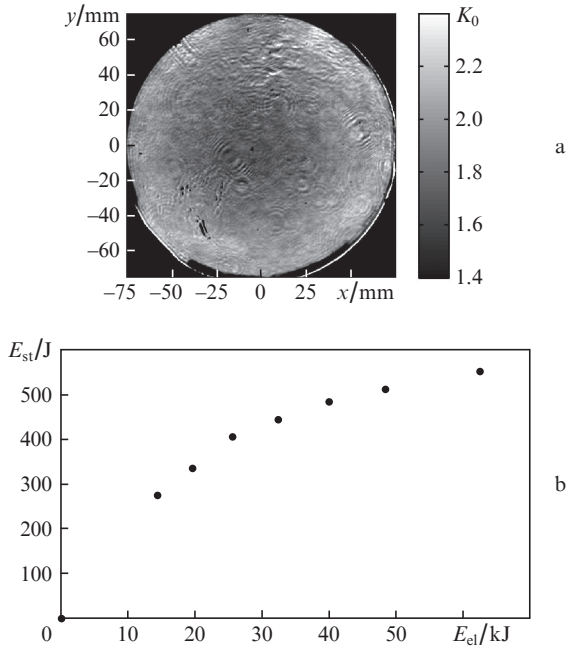

Figure 3. (a) Small-signal gain distribution over the amplifier aperture and (b) dependences of the energy stored in the amplifier on the electric energy in the capacitors.

4. Amplifier feasibility

As was already noted, the main factors limiting the pulse energy in neodymium glass lasers are optical breakdown and small-scale self-focusing. One more effect that should be taken into account is a temporal shift of the amplified pulse intensity maximum [8]. Due to the crucially inhomogeneous gain distribution in the AE, this shift is different in the near-axial region and at the periphery of the beam, because of which the use of the amplified beam for pumping a parametric amplifier may lead to a modulation of the petawatt pulse spectrum over the aperture.

To estimate the practical efficiency of the laser amplifier with an AE 150 mm in diameter, we performed numerical modulation of a nine-cascade pump laser of a PEARL-10 petawatt complex. As a basis, we used a seven-cascade pump laser of a PEARL complex [9, 10] [beam energy 300 J, form factor (aperture filling factor) 0.86, pulse duration at half maximum 1 ns], at the exit of which we added a spatial scaling filter, two studied laser amplifiers with an aperture of 150 mm, and a spatial filter between the amplifiers. In the simulation, we used the experimental small-signal gain distributions (see Fig. 3a) averaged over the angular coordinate. The numerical simulation was based on the solution of the balance equations for a pulsed laser amplifier obtained in [11]. To take into account the absorption, we divided the AE into n layers, whose total length was equal to the length of the illuminated part of the AE. Between the layers, we introduced absorption integrally equal to the absorption in the active element (from 4% to 6% in different AEs). In addition, we

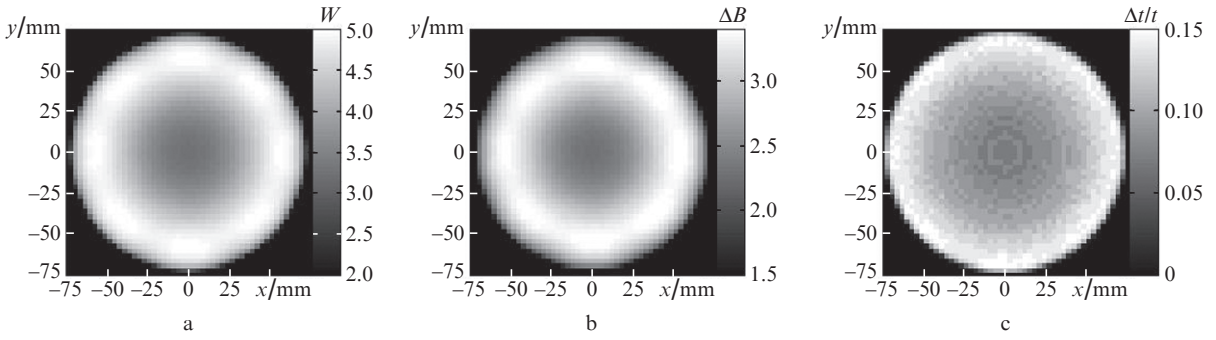

Figure 4. (a) Distributions of the output energy density, (b) *B*-integral increment and (c) shift of the intensity maximum of a pulse amplified in the final amplifier.

took into account the Fresnel losses. The diffraction effects and phase distortions in the AE were not taken into account in this calculation. The calculation results are given in Fig. 4.

As is seen from Fig. 4a, the energy density in the centre is lower than at the periphery. At the same time, the form factor is 0.83, which is only by 0.03 lower than for the beam incident on the amplifier. The output pulse energy is 620 J while the output energy of the previous cascade is 460 J, i.e., 230 J from 500 J stored in the amplifier are transferred to the output pulse. It should be emphasised that this calculation takes into account the energy losses for absorption in the glass and the Fresnel losses on the rod faces, which have no antireflection coating.

The increment of the *B*-integral in the process of beam propagation through the amplifier is shown in Fig. 4b. The maximum *B*, which is 3.4 for linear polarisation, can be decreased by using circular polarisation to be lower than the limiting value [5]. The inhomogeneity in the temporal shift of the pulse maximum (Fig. 4c) in the final amplifier does not exceed 1/20 of the pulse duration and, hence, cannot considerably deteriorate the parameters of the petawatt parametric amplifier. As a result, the addition of amplifiers 150 mm in diameter allows one to expect an increase in the parametric amplifier output energy up to 75 J, which corresponds to a power higher than 1 PW after the pulse compression.

5. Determination of the maximum pulse repetition rate

The feasibility and operability of a pulsed laser system depends on the pulse repetition rate. We studied the maximum possible increase in the repetition rate of pulses pumping the considered amplifier based on a neodymium phosphate glass rod 150 mm in diameter. The main initial data for these investigations are the changes in the temperature distribution caused by the pump pulses. The temperature distributions in amplifiers with diameters from 45 to 100 mm were determined in [4, 12–14] based on measured depolarisation. A characteristic feature of these distributions is the presence of two components: the first component, which relates to the quantum defect, in general coincides with the small-signal gain distribution and the second component depends on the absorption of the UV radiation of pump lamps and manifests itself in strong heating of narrow regions near the side surface of the rod,

$$\Delta T^{(0)} = \alpha G(r) + \beta \exp[(r - R)/\delta],$$

where r is the polar radius, R is the rod radius, $G(r)$ is the radial distribution of the small-signal gain, δ is the subsurface heat release factor, and α and β are coefficients. The coefficient α depends on the parameters of the electric discharge in the pump lamps and on the relation between the geometric dimensions of amplifier units (rod diameter, thickness of the cooling water layer, distance to the pump lamps, reflector type). The coefficient β is proportional to the radiation energy of the pump lamps per unit surface area of the AE. The considered amplifier with the rod 150 mm in diameter is similar in geometric proportions, reflector type, and pump lamp discharge characteristics to the studied previously amplifier [4, 13] with a diameter of 100 mm and the coefficients α_{100} = 0.32 K, β_{100} = 1.5 K, and δ_{100} = 2 mm (hereinafter, the subscript denotes the AE diameter). Taking into account that the electric discharge in each lamp remains the same, the number of lamps is doubled (16 instead of 8), and the rod diameter is increased by 1.5 times, we obtain $\beta_{150} = 2\beta_{100}/1.5 = 2$ K. In calculations, we assume that $\alpha_{150} = \alpha_{100}$ and $\delta_{150} = \delta_{100}$.

The validity of this concept is confirmed by good coincidence of the calculation results with the experimentally measured depolarisation pattern (Fig. 5).

In the repetitively pulsed regime, when the time from the beginning of a pulse series exceeds the relaxation time of the

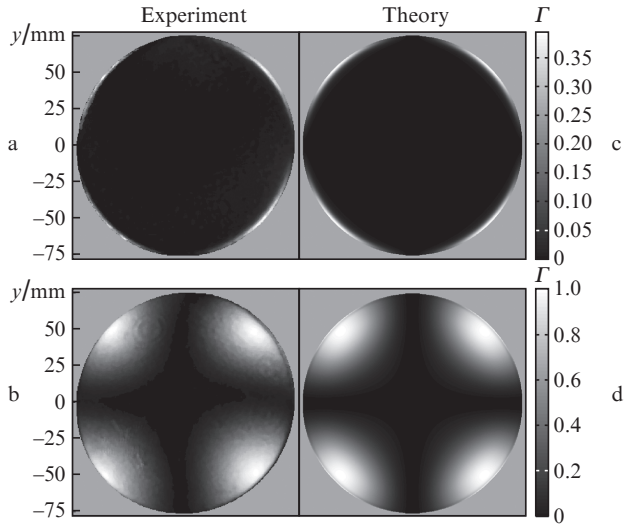

Figure 5. (a, b) Experimental and (c, d) calculated (by the proposed model) distributions of the depolarisation degree Γ in the AE 150 mm in diameter for a series of pump pulses with a repetition rate of one pulse per ten minutes (f = 0.0017 Hz) (a, c) after the first pulse and (b, d) in the steady-state regime.

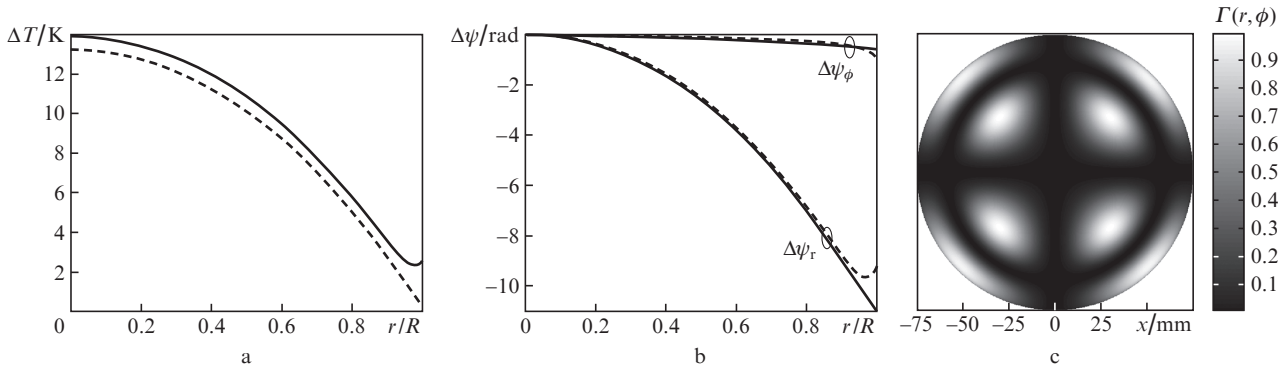

Figure 6. (a) Steady-state distributions of the temperature, (b) phase incursions of intrinsic waves in the AE immediately before (dashed lines) and after (solid lines) the pump pulse and (c) depolarisation degree calculated for $f = 0.0033$ Hz.

spatial zero mode of the temperature distribution (zero Bessel function with the lowest number of oscillations in the AE radius), the heat balance in the AE becomes steady state, i.e., the heat energy absorbed in the AE during a pump pulse becomes equal to the heat energy removed from the AE surface for the time between pulses. In calculations, we ignored longitudinal heat flows, which is true even for rather moderate flow rates of cooling liquid [15]. The results of calculations of depolarisation in an AE 150 mm in diameter for the pulse repetition rate $f = 0.0017$ Hz (one pulse per ten minutes) are given in Fig. 5d and demonstrate good agreement with the experimentally measured distribution (Fig. 5b). By numerically solving the thermal conductivity and elasticity equations, we determined the temperature and mechanical stress distributions. The calculations showed that, at the pump pulse repetition rate $f = 0.0033$ Hz (one pulse per five minutes), the stresses in the rod are five times weaker than the limiting stress, which causes breakdown of the AE (30 MPa [16]).

Figures 6a and 6b show the calculated radial temperature distributions ΔT and the phase increments of the radially and tangentially polarised waves $\Delta\psi_r$ and $\Delta\psi_\phi$ in the rod in the steady-state regime ($f = 0.0033$ Hz). These waves propagate in the AE with unchanged polarisation. The difference between their phase incursions $\delta = \Delta\psi_\phi - \Delta\psi_r$ determines the depolarisation degree Γ (ratio of the depolarised component intensity to the total radiation intensity at the AE exit). The $\Delta\psi_r$ and $\Delta\psi_\phi$ distributions in Fig. 6b are close to parabolic with the focal lengths F_r and F_ϕ equal to 1.5 and 30 km, respectively.

The steady-state depolarisation distribution over the rod aperture immediately after the pump pulse action calculated at $f = 0.0033$ is given in Fig. 6c. It is assumed that the beam at the entrance to the AE is linearly polarised. As is shown in [3], such thermally induced distortions can be effectively (to a level of 1%–2%) compensated using a 90° polarisation rotator placed between two amplifiers. As was mentioned above, at this pulse repetition rate, there exists a five-fold safety factor with respect to the AE breakdown threshold, which seems to be quite sufficient. Thus, the studied amplifier can be efficiently used at a pulse repetition rate of one pulse per five minutes.

6. Conclusions

An amplifier pump cavity with an active element of neodymium-doped phosphate glass (KGSS 0180) is developed. The AE has a diameter of 150 mm, a length of 320 mm, and a tilt angle of faces of 5°. The optical characteristics are measured to be as follows: the aperture-averaged small-signal gain at an electric pump energy of 48 kJ is 2.3, the energy stored at the laser transition is ~500 J, and the depolarisation in the case of single pump pulses does not exceed 0.2%. It is shown that the maximum pulse repetition rate for a five-fold safety factor with respect to the mechanical breakdown of the rod is one pulse per five minutes. In this case, depolarisation exceeds 25% but can be compensated to a level of 1%–2% by using a 90° polarisation rotator placed between two amplifiers. The use of this amplifier as a final cascade in the pump laser of a PEARL-10 complex being created in the Institute of Applied Physics, Russian Academy of Sciences, will allow one to obtain optical pulses with a duration of 1 ns and an energy exceeding 600 J. The *B*-integral in the final amplifier cascade does not exceed admissible values. The aperture of 150 mm is obviously the maximum possible for rod amplifiers.

Acknowledgements. This work was supported by the Programme of the Presidium of the Russian Academy of Sciences 'Extreme Light Fields and Their Applications'.

References

1. Bayanov V.I., Bordachev E.G., Volynkin V.M., Kryzhanovskii V.I., Mak A.A., Motorin I.V., Nikonova V.M., Serebryakov V.A., Starikov A.D., Charukhchev A.V., Shchavelev O.S., Yashin V.E. *Kvantovaya Elektron.*, **13** (9), 1891 (1986) [*Sov. J. Quantum Electron.*, **16** (9), 1240 (1986)].
2. Bayanov V.I., Bordachev E.G., Kryzhanovskii V.I., Serebryakov V.A., Shchavelev O.S., Charukhchev A.V., Yashin V.E. *Kvantovaya Elektron.*, **11** (2), 310 (1984) [*Sov. J. Quantum Electron.*, **14** (2), 213 (1984)].
3. Kuz'min A.A., Kulagin O.V., Khazanov E.A., Shaikin A.A. *Kvantovaya Elektron.*, **43** (7), 597 (2013) [*Quantum Electron.*, **43** (7), 597 (2013)].
4. Kuzmin A.A., Khazanov E.A., Shaykin A.A. *Opt. Express*, **19**, 14223 (2011).
5. Poteomkin A.K., Martyanov M.A., Kochetkova M.S., Khazanov E.A. *IEEE J. Quantum Electron.*, **45**, 336 (2009).
6. Poteomkin A.K., Khazanov E.A., Martyanov M.A., Kirsanov A.V., Shaykin A.A. *IEEE J. Quantum Electron.*, **45**, 854 (2009).
7. Poteomkin A.K., Zhurin K.A., Kirsanov A.V., Kopelovich E.A., Kuznetsov M.V., Kuz'min A.A., Flat F.A., Khazanov E.A., Shaikin A.A. *Kvantovaya Elektron.*, **41** (6), 487 (2011) [*Quantum Electron.*, **41** (6), 487 (2011)].
8. Mart'yanov M.A., Luchinin G.A., Poteomkin A.K., Khazanov E.A. *Kvantovaya Elektron.*, **38** (2), 103 (2008) [*Quantum Electron.*, **38** (2), 103 (2008)].
9. Lozhkarev V.V., Freidman G.I., Ginzburg V.N., Katin E.V., Khazanov E.A., Kirsanov A.V., Luchinin G.A., Mal'shakov A.N., Martyanov M.A., Palashov O.V., Poteomkin A.K., Sergeev A.M., Shaykin A.A., Yakovlev I.V. Preprint IAP No.720 (N.Novgorod, 2006).

10. Lozhkarev V.V., Freidman G.I., Ginzburg V.N., Katin E.V., Khazanov E.A., Kirsanov A.V., Luchinin G.A., Mal'shakov A.N., Martyanov M.A., Palashov O.V., Poteomkin A.K., Sergeev A.M., Shaykin A.A., Yakovlev I.V. *Laser Phys. Lett.*, **4**, 421 (2007).
11. Frantz L.M., Nodvik J.S. *J. Appl. Phys.*, **34**, 2346 (1963).
12. Kuz'min A.A., Luchinin G.A., Poteomkin A.K., Solov'ev A.A., Khazanov E.A., Shaikin A.A. *Kvantovaya Elektron.*, **39** (10), 895 (2009) [*Quantum Electron*., **39** (10), 895 (2009)].
13. Kuz'min A.A., Khazanov E.A., Shaikin A.A. *Kvantovaya Elektron*., **42** (4), 283 (2012) [*Quantum Electron*., **42** (4), 283 (2012)].
14. Kuzmin A.A., Silin D.E., Shaykin A.A., Kozhevatov I.E., Khazanov E.A. *J. Opt. Soc. Am. B*, **29** (6), 1152 (2012).
15. Mezenov A.V., Soms L.N., Stepanov A.I. *Termooptika tverdotel'nykh laserov* (Thermooptics of Solid-State Lasers) (Leningrad: Mashinostroenie, 1986).
16. Avakyants L.I., Buzhinskii I.M., Koryagina E.I., Surkova V.F. *Kvantovaya Elektron*., **5** (4), 725 (1978) [*Sov. J. Quantum Electron*., **8** (4), 423 (1978)].